

A fiber-optic Fabry-Perot pressure sensor with the $\text{Si}_3\text{N}_4/\text{SiO}_2/\text{Si}_3\text{N}_4$ diaphragm fabricated using micromachining technology

Myung-Gyoo Kim, Jaehee Park*, Shin-Won Kang**, and Byung-Ki Sohn**

Electronics & Telecommunications Research Institute, 161, Kajong-Dong, Yusong-Gu, Daejeon, Korea,

*Keimyung University, Dept. of Computer and Electronics Eng., 1000, Shindang-Dong, Dalseo-Gu, Daegu, Korea, **Sensor Technology Research Center, Kyungpook National University, 1370, San-Kyuk Dong, Puk-Gu, Daegu, Korea

Abstract

We have developed the high sensitivity fiber optic Fabry-Perot pressure sensor with a $\text{Si}_3\text{N}_4/\text{SiO}_2/\text{Si}_3\text{N}_4(\text{N/O/N})$ diaphragm fabricated using micromachining technology in the anisotropic etchant KOH solution. The configuration of this sensor was a 2 cm length fiber optic Fabry-Perot interferometer bonded to a 0.6 μm thick diaphragm. When the area of the N/O/N diaphragm used in the experiments was $2 \times 2 \text{ mm}^2$, the pressure sensitivity was 0.11 radian/kPa, and when the area was $8 \times 8 \text{ mm}^2$, the pressure sensitivity was increased to 1.57 radian/kPa. The phase change was dependent upon the applied pressure linearly.

Keywords: Anisotropic etching, $\text{Si}_3\text{N}_4/\text{SiO}_2/\text{Si}_3\text{N}_4$ diaphragm, and optical fiber pressure sensor

Introduction

Many fiber optic sensors, such as magnetic, acoustic, pressure, temperature, acceleration, gyro, displacement, current, and strain sensors, have been developed by researchers. These sensors possess several advantages over conventional sensors, including immunity to electromagnetic interference, rapid response, resistance to corrosion, and capability for remote sensing [1]. Recently, small size optical fiber pressure sensors for biomedical application were produced using micromachining technology. These sensors are classified into one of two general categories: intensity type sensor or interferometric type sensor. In the intensity type fiber optic pressure sensor [2], light is launched from the optical fiber, reflected at the micromachined diaphragm, and coupled into the optical fiber. When pressure is applied to the diaphragm, the diaphragm is deflected. The diaphragm deflection changes the light intensity coupled into the optical fiber. From the changes of coupling light intensity, pressure is measured. This sensor has low pressure sensitivity because the detection mechanism bases on the intensity variation. In the interferometric type sensor [3], the diaphragm and optical fiber end form a Fabry-Perot cavity whose length varies with pressure. Light is emitted from the optical fiber and reflected back at the

diaphragm. Then the light returns to the fiber from the diaphragm fabricated using micromachining technology. The light reflecting back into the fiber interferes with light reflected back from the end of fiber. When the diaphragm is subjected to pressure, the diaphragm deflection is induced. The induced diaphragm deflection causes the change of the Fabry-Perot cavity length and the phase change of the interference light. In the interferometric type fiber optic sensor, the short cavity length of the Fabry-Perot interferometer provides the low pressure sensitivity relatively. Besides, it has the difficulty in reading because of changes of the amplitude and the phase of the interferometric signal simultaneously due to the diaphragm deflection induced by the applied pressure. In this paper, we have investigated a fiber optic pressure sensor with high sensitivity produced by micromachining technology. The pressure sensor was configured as the fiber optic Fabry-Perot interferometer bonded to the surface of the N/O/N diaphragm made by micromachining technology.

Fiber Optic Fabry-Perot Interferometer

The fiber optic Fabry-Perot interferometer (FFPI) shown in Fig. 1 is composed of two internal mirrors spaced by a distance L . The light bounces back and forth between the mirrors, causing multiple-beam interference and hence fringes. With the assumptions that two mirrors are lossless and $R_{1,2}$ are the reflectances of two mirrors much less than 1 ($R_{1,2} \ll 1$), the ratio of reflected to incident optical power is

$$R_r = \frac{P_R}{P_{IN}} = R_1 + R_2 + 2\sqrt{R_1 R_2} \cos \phi \quad (1)$$

and the round trip phase difference in the interferometer is

$$\phi = \frac{4\pi n L}{\lambda} \quad (2)$$

where P_{IN} is the incident optical power, P_R is the reflected optical power, n is the effective refractive index, and λ is the optical wavelength. If $R_1 = R_2 = R$, the ratio formula becomes as follow:

$$R_r = 2R(1 + \cos \phi) . \quad (3)$$

The ratio of reflected and incident optical power is a function of the reflectances of two mirrors and the round trip phase difference, which depends on the optical length between two mirrors. As longitudinal strain applied to the FFPI, the round trip phase difference is shifted because of the change of the optical cavity length. The pressure-induced phase change [4] is

$$\delta\phi = 0.78 \times \frac{4\pi n(\delta L)}{\lambda} \quad (4)$$

where δL is the change of the cavity length of FFPI and 0.78 is a correction to account for the strain-optic effect.

Fabrication of sensing elements

The sensing element shown in Fig. 2 consists of a FFPI and a N/O/N diaphragm. The FFPI is produced with two single mode fibers coated on one end with a TiO₂ film [5]. The coated end of the first fiber is spliced to the uncoated fiber lead using a fusion splicing technique. The mirror reflectance is adjusted to the desired value by applying an appropriate number of splicing pulses with proper amplitude of the arc current. Usually, 10 to 20 splicing pulses with low arc current are needed. Then the first fiber is cleaved at a desired cavity length to attach the next mirror. Finally, the coated end of the second fiber is spliced to the cleaved end of the first fiber.

The fabrication sequence of a N/O/N diaphragm is illustrated in Fig. 3. First, 150 nm-Si₃N₄ / 300 nm-SiO₂ / 150 nm-Si₃N₄ (N/O/N) dielectric films are deposited on a 610 μm thick, 5", p-type, <100> oriented silicon wafer. Top and bottom layers are grown by low pressure chemical vapor deposition (LPCVD) at 780 $^{\circ}\text{C}$, and a mid-SiO₂ layer is grown by atmosphere pressure CVD (APCVD) at 380 $^{\circ}\text{C}$ under the SiH₄ and N₂O mixture gas ambient. This triple dielectric thin film has relatively stable mechanical stress characters and very low thermal conductivity [6], [7]. For protecting the N/O/N thin film and acting as the masking material during the reactive ion etching, the top and bottom surfaces of a silicon wafer deposited by a N/O/N thin film are coated with a positive photoresist (AZ 1512). After the photolithography process, the wet and dry etching are carried out for patterning the one surface of the N/O/N thin film. Finally, the wafer is anisotropically etched in the anisotropic etchant 44 wt.% KOH solution to the desired depth. In the anisotropic etching process, the N/O/N thin film acts as the masking material. Figure 4 shows the microphotograph of the N/O/N diaphragm produced by the fabrication procedures. The surface of the diaphragm was very clean and smooth, and was not covered by pyramid-like hillocks.

For making a sensing element used in the experiments, a 2 cm length FFPI and a 0.6 μm thick diaphragm was produced by the fabrication procedures. Moreover, the FFPI was bonded to the diaphragm with a small amount of epoxy.

Experimental setup and results

The experiment arrangement shown in Fig. 5 consists of a light source, a photodetector (PCO, RTZ-565-395), a 3-dB directional coupler (Canstar), a pulse generator, an oscilloscope, an air pump, and a digital manometer. The light source is a 1.3 μm single mode laser diode (Lasertron model QLM 3S855-02) whose threshold current is about 33 mA at room temperature. An air pump applies pressure to the silicon diaphragm and a digital manometer reads the pressure applied by a pump. The pulsed modulated light is emitted from a light source, propagated inside the fiber through a 3-dB coupler, and reached at a fiber optic Fabry-Perot interferometer. The interference is occurred at the FFPI, and the interference signal returns to a photodetector, and is converted to an electrical signal. The electrical signal is displayed on an oscilloscope. When the pressure is applied by a handpump, the diaphragm is deflected. The diaphragm deflection causes the FFPI to experience longitudinal strain. The longitudinal strain induces the optical length change of the FFPI. The length change produces the phase change of the interference signal.

Figure 6 is illustrated the response of a fiber optic pressure sensor with a silicon diaphragm fabricated by the micro machining technology. When the sizes of the N/O/N diaphragm were $2 \times 2 \text{ mm}^2$ and $8 \times 8 \text{ mm}^2$, the pressure sensitivities were 0.11 radian/kPa and 1.57 radian/kPa, respectively. These results show that the sensitivity increases as the diaphragm area increases and the phase change is dependent upon the applied pressure linearly. From our results, if the diaphragm with the other size and thickness is used, we anticipate a different pressure sensitivity. In addition, the longer the cavity length of the FFPI, the higher the pressure sensitivity.

Conclusions

We developed the high sensitivity fiber optic pressure sensor, which was configured as the FFPI attached to the N/O/N diaphragm used as a pressure transfer material. The $0.6 \text{ }\mu\text{m}$ thick diaphragm was produced by the anisotropic etching method with 44 wt.% KOH solution, and the 2 cm length FFPI was made with the uncoated fiber and the coated fiber with TiO_2 dielectric film. When the area of diaphragm was $2 \times 2 \text{ mm}^2$, the pressure sensitivity was 0.11 radian/kPa, and when the area of $8 \times 8 \text{ mm}^2$ was used, the pressure sensitivity was 1.57 increased to radian/kPa. The experiment results showed that the phase change is varied with the applied pressure linearly.

References

- [1] T. Giallorenzi, J. Bucaro, A. Dandridge, G. Sigel, J. Cole, S. Rashleigh, and R. Priest, "Optical fiber sensor technology," *IEEE J. Quantum Electron.*, vol. 20, pp. 626~665, 1982.
- [2] O. Tohyama, M. Kohashi, K. Yamamoto, and H. Itoh, "A fiber-optic silicon pressure sensor for ultra-thin catheters," *Transducers '95*, pp. 596~599, 1995.
- [3] M. Chan, S. Collins, and R. Smith, "A micromachined pressure sensor with fiber-optic interferometric readout," *Sensor and Actuators A*, vol. 43, pp. 196~201, 1994.
- [4] R. Atkins, J. Gardner, W. Gibler, C. Lee, M. Oakland, M. Spears, V. Swenson, H. Taylor, J. McCoy, and G. beshouri, "Fiber-optic pressure sensors for internal combustion engines," *Applied Optics*, vol. 33, pp. 1315~1320, 1994.
- [5] C. Lee and H. Taylor, "Interferometric optical fiber sensors using internal mirrors," *Elec. Lett.*, vol. 24, pp. 193~194, 1988.
- [6] F. Völklein, "Thermal conductivity and diffusivity of a thin film $\text{SiO}_2\text{-Si}_3\text{N}_4$ sandwich system," *Thin Solid Film*, vol. 88, pp. 27~33, 1990.
- [7] Myung-Gyoo Kim, Dong-Su Park, Chang-Won Kim, Jin-Sup Kim, Jung-Hee Lee, Jong-Hyun Lee, Byung-Ki Sohn, "Fabrication of stress-balanced $\text{Si}_3\text{N}_4/\text{SiO}_2/\text{Si}_3\text{N}_4$ dielectric membrane," *J. Korea Sensors Society*, vol. 4, no. 3, pp. 51~59, 1995.

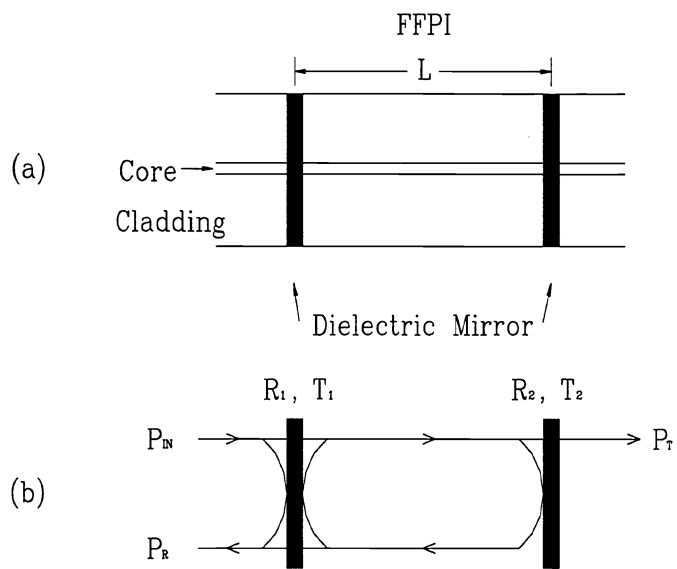


Fig. 1. A fiber optic Fabry-Perot interferometer with two internal mirrors:

(a) a cross-sectional view (b) operating principles.

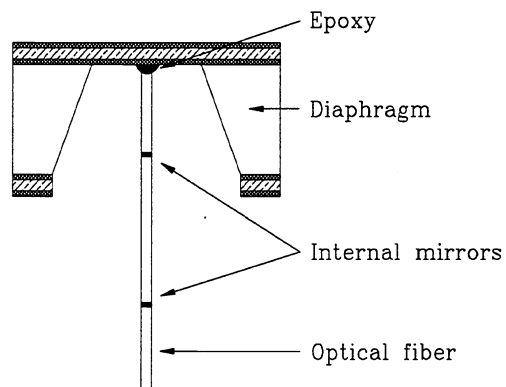


Fig. 2. A Sensing element.

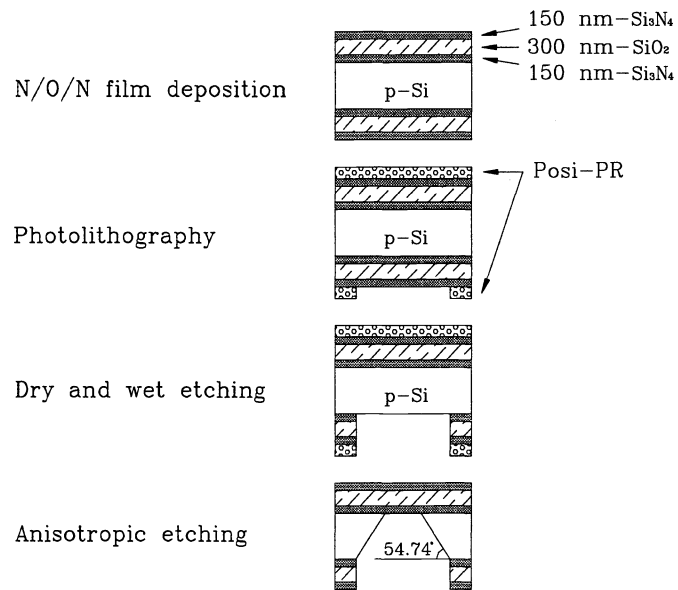


Fig. 3. Process sequence for fabrication of the N/O/N diaphragm.

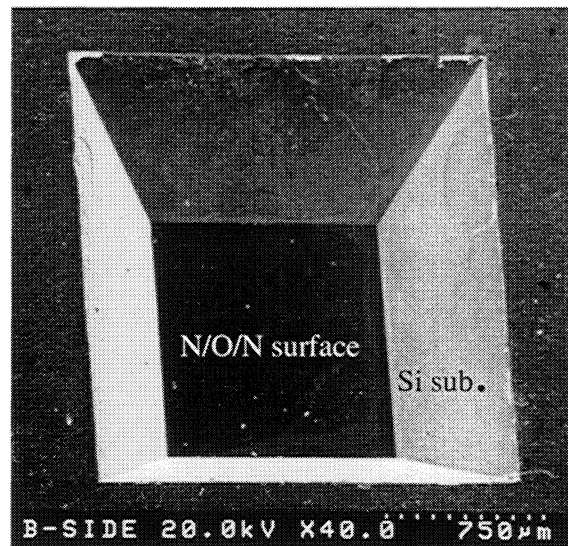


Fig. 4. Scanning electron microphotograph of diaphragm.

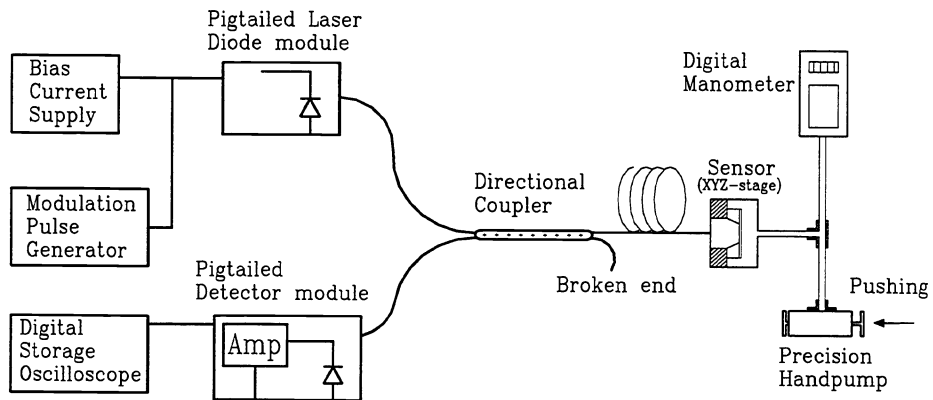


Fig. 5. Experimental setup for fiber optic pressure sensor.

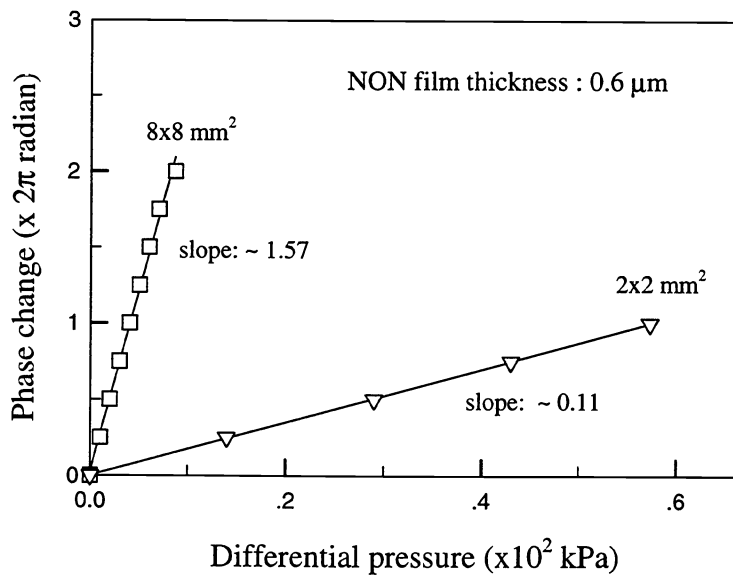


Fig. 6. Pressure characteristics on the N/O/N diaphragm size under longitudinal direction and

compressive stress.